Article

Oxepane Nucleic Acids: Synthesis, Characterization, and Properties of Oligonucleotides Bearing a Seven-Membered Carbohydrate Ring

David Sabatino, and Masad J. Damha

J. Am. Chem. Soc., **2007**, 129 (26), 8259-8270• DOI: 10.1021/ja071336c • Publication Date (Web): 09 June 2007

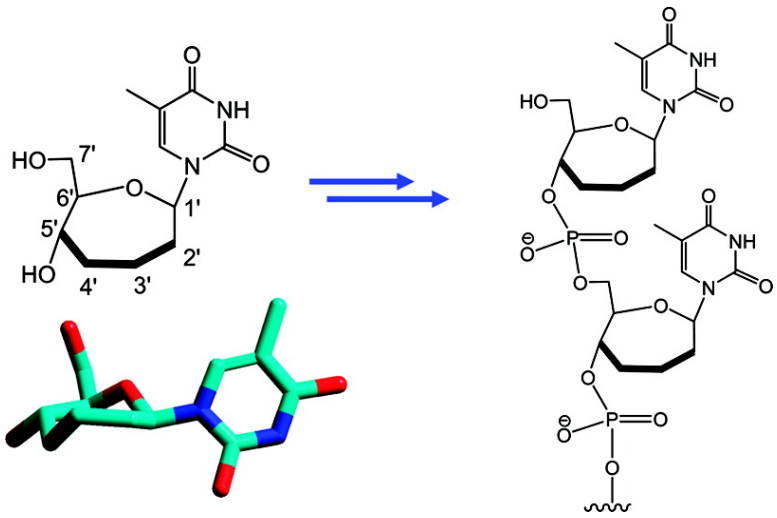

More About This Article

Additional resources and features associated with this article are available within the HTML version:

- Supporting Information
- Links to the 2 articles that cite this article, as of the time of this article download
- Access to high resolution figures
- Links to articles and content related to this article
- Copyright permission to reproduce figures and/or text from this article

View the Full Text HTML

J|A|C|S
ARTICLES
Published on Web 06/09/2007

Oxepane Nucleic Acids: Synthesis, Characterization, and Properties of Oligonucleotides Bearing a Seven-Membered Carbohydrate Ring

David Sabatino and Masad J. Damha*

Contribution from the Department of Chemistry, McGill University, 801 Sherbrooke Street West, Montreal, Quebec H3A 2K6, Canada

Received February 25, 2007; E-mail: masad.damha@mcgill.ca

Abstract: The synthesis and properties of oxepane nucleic acids (ONAs) are described. ONAs are sugar−phosphate oligomers in which the pentofuranose ring of DNA and RNA is replaced with a seven-membered (oxepane) sugar ring. The oxepane nucleoside monomers were prepared from the ring expansion reaction of a cyclopropanated glycal, **1**, and their conversion into phosphoramidite derivatives allowed efficient assembly of ONAs on a solid support. ONAs (oT_{15} and oA_{15}) were found to be much more resistant toward nuclease degradation than natural DNA (dT_{15} and dA_{15}) in fetal bovine serum (FBS) after 24 h of incubation at 37 °C. ONAs also display several attributes in common with the naturally occurring DNA. For example, oT_{15} exhibited cross-pairing with complementary RNA to give a duplex (oT_{15}/rA_{15}) whose conformation evaluated by CD spectroscopy very closely matched that of the natural DNA/RNA hybrid (dT_{15}/rA_{15}). Furthermore, oT_{15} was found to elicit *Escherichia coli* RNase H-mediated degradation of the rA_{15} strand. When we compared the rates of RNase H-mediated degradation induced by 5- (furanose, dT_{15}), 6- (2′-enopyranose, pT_{18}), and 7-membered (oxepane, oT_{15}) ring oligonucleotides at a temperature that ensures maximum duplex population (10 °C), the following trend was observed: $dT_{15} \gg oT_{15} > pT_{18}$. The wider implications of these results are discussed in the context of our current understanding of the catalytic mechanism of the enzyme. The homopolymer oT_{15} also paired with its oxepane complement, oA_{15}, to form a duplex structure that was different [as assessed by circular dichroic (CD) spectroscopy] and of lower thermal stability relative to the native dT_{15}/dA_{15} hybrid. Hence, ONAs are useful tools for biological studies and provide new insights into the structure and function of natural and alternative genetic systems.

Introduction

Oligonucleotide (ON) analogues are important for purposes of structural studies as well as potential therapeutic agents for gene silencing applications associated with antisense-,[1] antigene-,[2] RNAi-,[3] and aptamer[4] based modalities. In the optimal case for antisense ONs gene silencing occurs catalytically in concert with a constitutive ribonuclease H (RNase H) enzyme capable of recognizing and understanding the mechanisms of substrate recognition by RNase H provides guidance to the design of future ONs for therapeutic use.[5]

We recently synthesized chimeric ONs composed of 2′-deoxy-2′-fluoro-β-D-arabinose or 2′-β-D-deoxyribose sugars with interspersed acyclic (e.g., 2′,3′-seconucleotide or butyl) residues.[6] These compounds combined both preorganization (fluoroarabinose moiety) and flexibility (acyclic linker moiety) within the host duplex, leading to very efficient RNase H-mediated cleavage of the complementary RNA. These studies indicated that enhanced flexibility of the ON backbone enables better alignment of the ON/RNA hybrid into the active site of RNase H, thereby conferring accelerated enzyme-catalyzed degradation of RNA.[7,8] To further test this hypothesis, we turned our attention to ON backbones that lack the furanose ring altogether but that would be flexible enough to adjust to the required duplex trajectory for RNase H recognition and cleavage.

Herein we describe the synthesis of nucleosides and oligonucleotides containing unsaturated 6-membered and saturated 7-membered ring structures, termed 2′-enopyranose and oxepane nucleic acids (ONA), respectively.[9] The ONAs (e.g., oT_{15}) were compared with native DNA (e.g., dT_{15}) and unsaturated 6-membered (e.g., pT_{18}) ring structures in terms of their ability to self-associate (e.g., oT_{15}/oA_{15}), cross-pair with native structures (e.g., oT_{15}/dA_{15} and oT_{15}/rA_{15}), and elicit RNase H-

(1) Minshull, J.; Hunt, T. *Nucleic Acids Res.* **1986,** *14*, 6433−6451.
(2) Le Doan, T.; Perrouault, L.; Praseuth, D.; Habhoub, N.; Decout, J. L.; Thoung, N. T.; Lhomme, J.; Helene, C. *Nucleic Acids Res.* **1987**, *15*, 7749−7760.
(3) Sontheimer, E. J.; Carthew, R. W. *Science* **2004**, *305*, 1409−1410.
(4) Shoji, A.; Kuwahara, M.; Ozaki, H.; Sawai, H. *J. Am. Chem. Soc.* **2007**, *129* (5), 1456−1464.
(5) Itaya, M.; Kondo, K. *Nucleic Acids Res.* **1991**, *19*, 4443−4449.
(6) Mangos, M. M.; Min, K.-L.; Viazovkina, E.; Galarneau, A.; Elzagheid, M. I.; Parniak, M. A.; Damha, M. J. *J. Am. Chem. Soc.* **2003**, *125* (3), 654−661.
(7) (a) Mangos, M. M.; Damha, M. J. *Curr. Top. Med. Chem.* **2002**, *2* (10), 1147−1171. (b) Yazbeck, D. R.; Min, K.-L.; Damha, M. J. *Nucleic Acids Res.* **2002**, *30* (14), 3015−3025.
(8) Verbeure, B.; Lescrinier, E.; Wang, J.; Herdewijn, P. *Nucleic Acids Res.* **2001**, *29* (24), 4941−4947.
(9) We had previously attempted to synthesize unsaturated heptose (i.e., oxepine) nucleic acids; however, isolation of the oligonucleotides was prevented by degradation of the oxepine-modified oligonucleotide during alkaline cleavage of the oligonucelotide from the succinyl linker solid support (D. Sabatino and M. J. Damha, unpublished results).

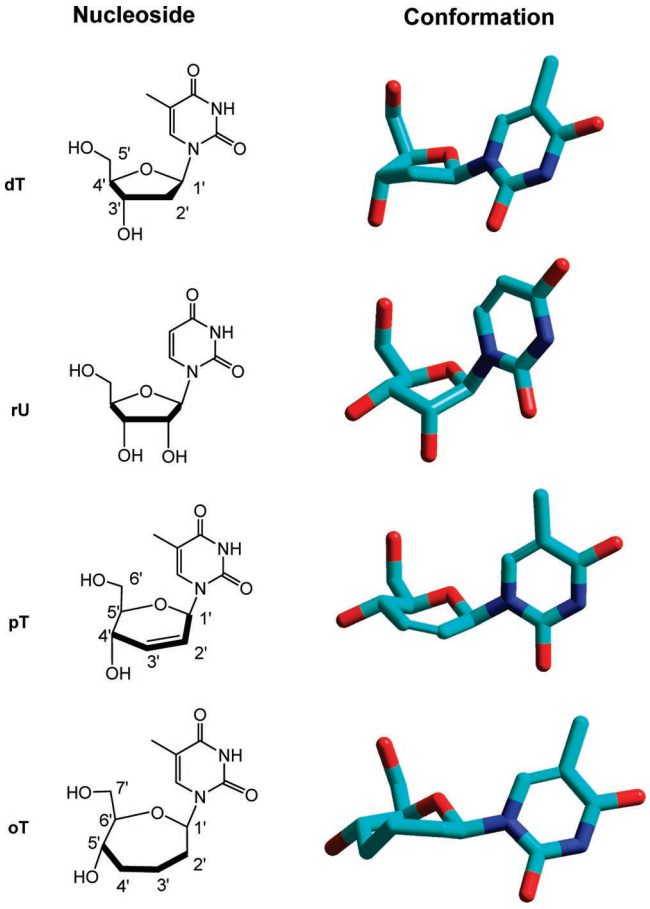

Figure 1. Structures and conformations of nucleosides.

mediated cleavage of their target RNA (rA_{15}). We show that the trend relating flexibility and RNase H activity persists at a temperature ensuring a maximum duplex population (10 °C) when we compare the RNase H activity of 5- (furanose, dT_{15}), 6- (2′-enopyranose, pT_{18}), and 7-membered (oxepane, oT_{15}) ring oligonucleotides with the flexibility of the constituent sugar rings (i.e., furanose[10] (5) > oxepane[11] (7) > 2′-enopyranose[12] (6) (Figure 1)]. In addition, oT_{15} and oA_{15} were found to be completely stable in fetal bovine serum after 24 h of incubation at 37 °C. These findings are significant in that they contribute to our knowledge about what types of chemical modifications are tolerated in an oligonucleotide strand for the development of RNase H-active, nuclease-stable ONs and their antisense applications.

Results and Discussion

To date, the largest expansion of the sugar moiety in DNA is that reported for six-membered ring hexopyranosyl nucleic acids and their assembly into (4′ → 6′) linked oligo(2′,3′-dideoxy-β-D-glucopyranosyl)nucleotides (i.e., "homo-DNA").[13,14] This architecture exhibits much stronger Watson−Crick base pairing than DNA, but it does not cross-pair with native DNA or RNA strands. The reason for this tighter base pairing was postulated to be a consequence of the higher rigidity of a pyranose compared to a furanose ring, resulting in a preorganization of the single strand's backbone conformation favoring a compact quasi-linear duplex.[14,15] Since then, more flexible unsaturated six-membered ring nucleic acids (e.g., cyclohexene NA) have been developed to promote binding to the natural systems in hybrid conformations that mimic the native duplexes.[16] Alternatively, contracting the carbohydrate moiety to a four-carbon skeleton, as in the α-L-threofuranosyl sugar, maintains a furanose half-chair sugar pucker conformation similar to native systems, allowing α-L-threofuranosyl nucleic acids, TNAs, to pair with its complement as well as to single-stranded ssDNA and ssRNA.[17,18] Here we report the synthesis and characterization of ONs bearing a 6- or 7-membered carbohydrate ring in place of the normal 5-membered ribofuranose ring.[9] We surmised that these relatively unconstrained ONs would exhibit RNase H induction properties as well as provide some insight toward elucidating the structural factors that provide the "optimal" ON/RNA substrate of the enzyme.[7,8]

Conformational Analysis. Molecular modeling of nucleoside conformation is commonly used to study carbohydrate geometry in duplex structures.[19] To gain insight into the conformation of oxepane and 2′-enopyranose oligomers, we conducted comparative computational analyses of the thymine nucleosides, oT and pT, along with the native nucleosides dT and rU (Figure 1).

Unsaturated 6-membered rings have been shown to be most stable in their twisted half-chair conformations with barriers to interconversion of 8−12 kcal/mol, oscillating predominantly via the boat (bent) conformation.[12,20] The nucleoside pT favors a $^{\circ}H_{5'}$ half-chair conformation such that the dihedral angle about the C4′−C5′ bond in the 2′-enopyranose ($\delta = 85°$) falls within the range of ribose in A-RNA-type helices (C3′−C4′, $\delta = 77°-97°$) (Figure 1).[21] The pseudorotational equilibrium for oxepane carbohydrates is more complex and involves many low-energy transitions between the boat (B), twist boat (TB), chair (C), and the favored twist chair (TC) forms.[11,22] The most common transition from C to TC geometry proceeds with relatively low interconversion energy barriers of 0.5−2 kcal/mol, whereas some of the less populated TC to B or B to TB transitions have interconversion energy barriers of 5−10 kcal/mol.[11] An ab initio geometry optimization was performed on oT nucleoside, **6**, in vacuo, with the 3-21 G basis set using HyperChem version 7.0. The Polak-Ribiere conjugate gradient algorithm was used, with a root-mean-square gradient termination cutoff of 0.05 kcal $Å^{-1}$ mol^{-1}. The calculations provided compact energy-minimized structures where the heptose carbohydrate was found to be either

(10) Gabb, H. A.; Harvey, S. C. *J. Am. Chem. Soc.* **1993**, *115*, 4218−4227.
(11) Espinosa, A.; Gallo, M. A.; Entrena, A.; Gomez, J. A. *J. Mol. Struct.* **1994**, *323*, 247−256.
(12) Choo, J.; Lee, S.-N.; Lee, K.-H. *Bull. Kor. Chem. Soc.* **1996**, *17* (1), 7−11.
(13) (a) Augustyns, K.; Vandendriessche, F.; Van Aerschot, A.; Busson, R.; Urbanke, C.; Herdewijn, P. *Nucl. Acids Res.* **1992**, *20*, 4711−4716. (b) Augustyns, K.; Van Aerschot, A.; Urbanke, C.; Herdewijn, P. *Bull. Soc. Chim. Belg.* **1992**, *101*, 119−130. (c) Hunzinker, von J.; Roth, H-J.; Bohringer, M.; Giger, A.; Diederichsen, U.; Gobel, M.; Krishnan, R.; Jaun, B.; Leumann, C.; Eschenmoser, A. *Helv. Chim. Acta.* **1993**, *76*, 259−352.
(14) Eschenmoser, A. *Science* **1999**, *284*, 2118−2124.
(15) Lescrinier, E.; Froeyen, M.; Herdewijn, P. *Nucleic Acids Res.* **2003**, *31* (12), 2975−2989.
(16) Wang, J.; Verbeure, B.; Luyten, I.; Lescrinire, E.; Froeyen, M.; Hendrix, C.; Rosemeyer, H.; Seela, F.; Van Aershot, A.; Herdewijn, P. *J. Am. Chem. Soc.* **2000**, *122*, 8595−8602.
(17) Schoning, K.-U.; Scholz, P.; Guntha, S.; Wu, X.; Krishnamurthy, R.; Eschenmoser, A. *Science* **2000**, *290* (5495), 1347−1351.
(18) Wilds, C. J.; Wawrzak, Z.; Krishnamurthy, R.; Eschenmoser, A.; Egli, M. *J. Am. Chem. Soc.* **2002**, *124*, 13716−13721.
(19) Noy, A.; Perez, A.; Marquez, M.; Luque, J.; Orozco, M. *J. Am. Chem. Soc.* **2005**, *127*, 4910−4920.
(20) (a) Ferrier, R. J.; Sankey, G. H. *J. Chem. Soc. C* **1966**, 2345−2349. (b) Laane, J.; Choo, J. *J. Am. Chem. Soc.* **1994**, *116*, 3889−3891.
(21) Felder, E.; Gattlen, R.; Ossola, F.; Baschang, G. *Nucleosides Nucleotides* **1992**, *11* (9), 1667−1671.
(22) DeMatteo, M. P.; Snyder, N. L.; Morton, M.; Baldisseri, D. M.; Hadad, C. M.; Peczuh, M. W. *J. Org. Chem.* **2005**, *70*, 24−38.

Scheme 1. Synthesis of Oxepane Nucleosides and Phosphoramidites[a]

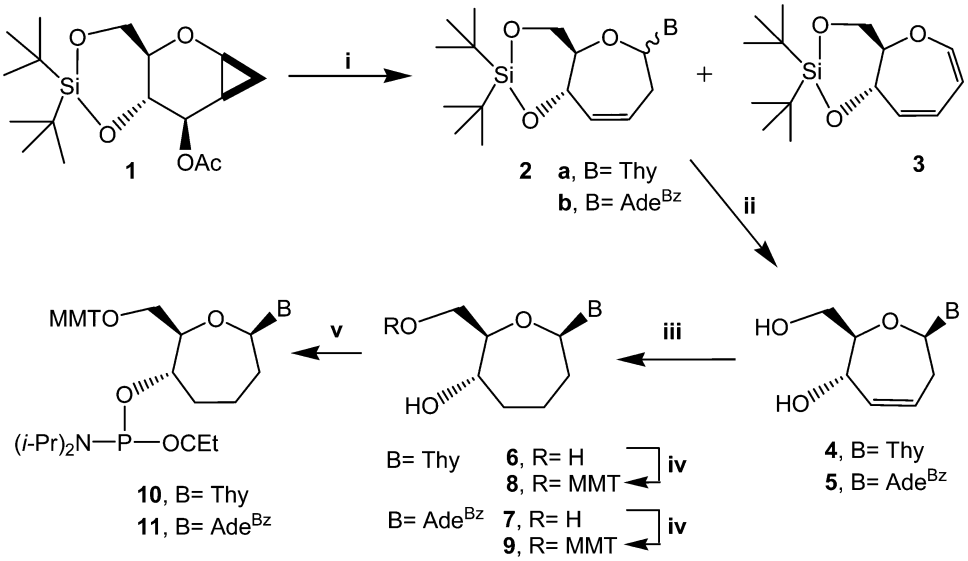

[a] Conditions and reagents: (i) persilylated base, TMSOTf, MeCN, reflux, 12−24 h, Thy 40% and Ade^{NBz} 45%; (ii) 1 M TBAF/THF, 0 °C, 1 h, Thy 90% and Ade^{NBz} 61%; (iii) 1 atm H_2, Pd/C, MeOH, 22 °C, 4 h, Thy 70% and Ade^{NBz} 99%; (iv) MMTCl, pyridine, 22 °C, 3 h, Thy 66% and Ade^{NBz} 50%; (v) ClP(OCEt)N(*i*-Pr)$_2$, EtN(*i*-Pr)$_2$, THF, 22 °C, 2 h, Thy 80% and Ade^{NBz} 90%.

in a chair or slightly twisted chair conformation ($^{O'6'}TC_{4'5'}$), with C4′ and C5′ lying below and the ring oxygen and C6′ above the plane of the molecule defined by C1′−C2′−C3′ (Figure 1).

Comparison of the oT conformation with the C2′-*endo*[23] sugar pucker of dT (Figure 1) revealed an expanded oxepane carbohydrate structure in which the in-ring diameter of oT is extended relative to the pentofuranose ring by 0.8 Å (i.e., for oT, C1′−C5′ = 3.11 Å, and for dT, C1′−C4′ = 2.35 Å), while the O−O distance in oT was found to be reduced by almost 0.8 Å (i.e., for oT, C7′OH−C5′OH = 3.57 Å, and for dT, C5′OH−C3′OH = 4.26 Å). Therefore, from this perspective, the oxepane modification provides a more compact oligonucleotide structure that can, in principle, hybridize to DNA and, even more favorably, to the more compact C3′-*endo*[23] geometry of RNA (i.e., for oT, C7′OH−C5′OH = 3.35 Å, and for rU, C5′OH−C3′OH = 3.80 Å) (Figure 1). However, two factors may limit the base-pairing potential of ONA with complementary DNA and RNA: (a) the increased ring size of the oxepane ring, as observed with pyranose-based ONs,[14,24] and (b) the relative orientation of the glycosidic bond (C1′−N1) with respect to the C5′−OH bond (Figure 1).[25]

Synthesis and Characterization of Nucleosides and Oligonucleotides. The oxepane nucleosides, oT and oA, were prepared by a procedure similar to the ring expansion reaction of cyclopropanated glycal sugars reported by Hoberg[26] (Scheme 1). We have expanded the scope of this reaction to nucleoside synthesis by introducing silylated thymine and N^6-benzoyladenine as nucleophiles. Thus, Vorbrüggen-type[27] glycosylation reactions with sugar **1** afforded the unsaturated oxepine nucleoside, **2**, along with the diene byproduct, **3**. The product distribution for the reaction was found to be dependent on the potency of the nucleophile (Table 1). Coupling with N^6-benzoyladenine proceeded more rapidly and more efficiently than with thymine (0.5 day vs 1 day reflux) at the expense of a poorer diastereoselectivity (2:1 β:α for N^6-benzoyladenine and 10:1 β:α for thymine). The β- and α-anomeric configurations of the nucleosides were unequivocally established by NOESY experiments (see Supporting Information Figure S16). Following desilylation and reduction of the double bond, the oxepane 5′-*O*-phosphoramidite derivatives **10** and **11** were prepared and purified by standard methods (Scheme 1). While the dimethoxytrityl protecting group is more commonly used in ON synthesis, we chose the 5′-MMT group as it is more stable and, in our hands provides higher yield of nucleosides.

Table 1. Selectivity of the Glycosylation Reaction of **1**

Base		Stereoselectivity (β:α)	Chemoselectivity (2 vs 3)
Thy	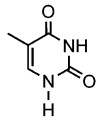	10:1	1.3 : 1 40% : 30%
Ade^{NBz}	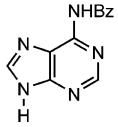	2:1	3 : 1 45% : 15%

The synthesis of the unsaturated pyranose nucleoside, pT, and its corresponding phosphoramidite was accomplished with a slightly modified procedure,[28] starting from commercially available tri-*O*-acetyl-D-glucal (Scheme 2). The reaction of silylated thymine with tri-*O*-acetyl-D-glucal in the presence of Lewis acid catalyst TMSOTf proceeded to completion by refluxing in MeCN for 3 h.

(23) (a) Pauling, L.; Corey, R. B. *Proc. Natl. Acad. Sci. U.S.A.* **1953**, *39* (2), 84−97. (b) Allen, F. H.; Kennard, O.; Watson, D. G.; Brammer, L.; Orpen, A. G.; Taylor, R. *J. Chem. Soc., Perkin Trans. 2* **1987**, S1−S19. (c) Gelbin, A.; Schneider, B.; Clowney, L.; Hsieh, S.-H.; Olson, W. K.; Berman, H. M. *J. Am. Chem. Soc.* **1996**, *118*, 519−529.
(24) Kerremans, L.; Schepers, G.; Rozenski, J.; Busson, R.; Van Aerschot, A.; Herdewijn, P. *Org. Lett.* **2001**, *3* (26), 4129−4132.
(25) Premraj, B. J.; Yathindra, S. R. N. *Biophys. Chem.* **2002**, *95*, 253−272.
(26) Hoberg, J. O. *J. Org. Chem.* **1997**, *62* (19), 6615−6618.
(27) Skalmowski, B. B.; Krolikiewicz, K.; Vorbruggen, H. *Tetrahedron Lett.* **1995**, *36* (43), 7845−7848.
(28) Pedersen, H.; Perdersen, E. K. *Heterocylces* **1992**, *34* (2), 265−272.

Scheme 2. Synthesis of 2′-Enopyranosyl Nucleoside *O*-Phosphoramidites[a]

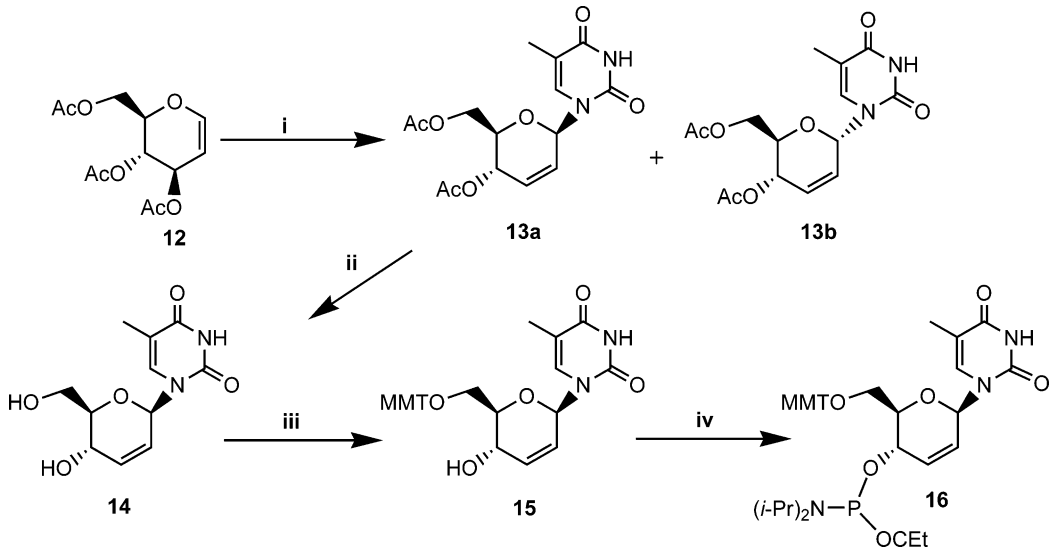

[a] Reagents and conditions: (i) bis(trimethylsilyl)thymine, TMSOTf, MeCN, reflux, 3 h (75%); (ii) 0.1 M NaOMe/MeOH 1 h, (93%); (iii) MMTCl, pyridine, 22 °C, 3 h (78%); (iv) $ClP(OCEt)N(i\text{-}Pr)_2$, $EtN(i\text{-}Pr)_2$, THF, 22 °C, 1 h (80%).

The reaction after purification yielded 75% **13** in a separable 1.1:1 ratio in α:β diastereoselectivity at the anomeric C1′-position. The structures of **13a** and **13b** were confirmed by ^1H and ^{13}C NMR, and the chemical shift data obtained were in complete agreement with the literature data.[29] Nucleoside **13a** was subsequently treated with 0.1 M NaOMe/MeOH to yield the completely deprotected nucleoside **14** in a $^{\circ}H_{5'}$ half-chair conformation as identified by the characteristic coupling constants, that is, $J_{1'2'} \sim 1$ Hz and $J_{4'5'} = 6.8$ Hz (see Experimental Section).[29] The nucleoside was monomethoxytritylated at the primary C6′ hydroxyl and then treated with $Cl\text{-}P(OCEt)N(i\text{-}Pr)_2$ to yield the phosphoramidite **16**, suitable for solid-phase oligonucleotide synthesis.

The homopolymeric oT_{15}, oA_{15}, and pT_{18} strands were assembled on a commercially available 500 Å long-chain alkylamino Unylinker CPG support.[30] With a limited supply of oT and oA monomers in hand, phosphoramidites **10** and **11** were used as 0.05 M solutions (in anhydrous CH_2Cl_2 for **10** and in anhydrous MeCN for the more polar nucleoside **11**). Oligonucleotide syntheses were conducted on a 0.5 μmol scale with extended amidite coupling times (30 min) and 5-ethylthiotetrazole, ETT, as the activator (0.25 M in MeCN). The detritylation step was extended to 2.5 min in order to ensure complete removal of the monomethoxytrityl (MMT) group. All other sequences were synthesized by conventional procedures.[31] The desired oligonucleotides (i.e., oT_{15}, oA_{15}, and pT_{18}) constituted 65−70% of the crude material isolated after deprotection (see Supporting Information Figures S1 and S2), indicating that under the conditions used, the monomers coupled with 98−99% efficiency. Recoveries of oT_{15} and oA_{15} from the solid support were ca. 25 OD units (25−40% yield). Following purification by HPLC and/or denaturing PAGE conditions, the oligomers were desalted by size-exclusion chromatography (Sephadex G-25). The structure of the oligonucleotides was confirmed by MALDI-TOF mass spectrometry (see Supporting Information Table S1).[32]

Table 2. Comparison of UV Thermal Melt and Percent Hyperchromicity Values for Pairing and Cross-Pairing of 2′-Enopyranose (pT) and Oxepane (oT and oA) Oligonucleotides and Control DNA (dT and dA) and RNA (rU and rA) Sequences[a]

sequences	T_m (°C)	% H
1. $oT_{15} + oA_{15}$	12[b]	4.5
2. $oT_{15} + dA_{15}$	<5	8.7
3. $oT_{15} + rA_{15}$	13[b]	11.3
4. $dT_{15} + oA_{15}$	<5	3.3
5. $rU_{15} + oA_{15}$	12[b]	3.4
6. $pT_{18} + dA_{18}$	34[b]	11.3
7. $pT_{18} + rA_{18}$	25[b]	15.3
8. $dT_{15} + dA_{15}$	37	24.8
9. $dT_{15} + rA_{15}$	32	25.4
10. $rU_{15} + rA_{15}$	25	28.7
11. $rU_{15} + dA_{15}$	16	20.7

[a] Duplex concentration of 3.04 μM in sodium phosphate buffer: 140 mM KCl, 1 mM $MgCl_2$, and 5 mM Na_2HPO_4 adjusted to pH = 7. [b] Early and/or broad transition curve.

Hybridization Properties of Oxepane-Modified Oligonucleotides. 1. oT_{15}/oA_{15} Duplex. Hybridization of oligonucleotide strands was first assessed by UV-monitored thermal denaturation experiments; phosphate buffers typically contained 1 mM Mg^{2+} and 5 mM Na^+ (see Experimental Section) and were maintained at pH = 7 (Table 2 lists the sequences that were investigated). As anticipated from previous studies,[33,40] the control duplexes dT_{15}/dA_{15}, rU_{15}/rA_{15}, dT_{15}/rA_{15}, and rU_{15}/dA_{15} all exhibited a single-phase transition with 20−30% hyperchromicity (Table 2). By contrast, binding experiments on oT_{15}/oA_{15} showed a weak but clearly detectable early transition curve ($T_m = 12$ °C) (Figure 2B). In addition, changes in hyperchromicity (% H), were quite small, suggesting the formation of a weaker complex relative to the native duplex

(29) (a) Herscovici, J.; Montserret, R.; Antonakis, K. *Carbohydr. Res.* **1988**, *176*, 219−229. (b) Doboszewski, B.; Blaton, N.; Herdewijn, P. *J. Org. Chem.* **1995**, *60*, 7909−7919.
(30) Guzaev, A. P.; Manoharan, M. *J. Am. Chem. Soc.* **2003**, *125*, 2380−2381.
(31) (a) Caruthers, M. H.; Barone, A. D.; Beaucage, S. L.; Dodds, D. R.; Fisher, E. F.; McBride, L. J.; Mateucci, M.; Stabinsky, Z.; Tang, Y.-J. *Methods Enzymol.* **1987**, *154*, 287−313. (b) Damha, M. J.; Ogilvie, K. K. *Methods Mol. Biol.* **1993**, *20*, 81−114.
(32) Distler, A. M.; Allison, J. *Anal. Chem.* **2001**, *73*, 5000−5003.
(33) (a) Kim, K.; Jhon, M. S. *Biochim. Biophys. Acta* **1979**, *565*, 131−147. (b) Aymaan, J.; Coll, M.; Frederick, C. A.; Wang, A. H.-J.; Rich, A. *Nucleic Acids Res.* **1989**, *17*, 3229−3245. (c) Hall, K. B.; McLaughin, L. W. *Biochemistry* **1991**, *30*, 10606−10613. (d) Ratmeyer, L.; Vinayak, R.; Zhong, Y. Y.; Zon, G.; Wilson, W. D. *Biochemistry* **1994**, *33*, 5298−5304.

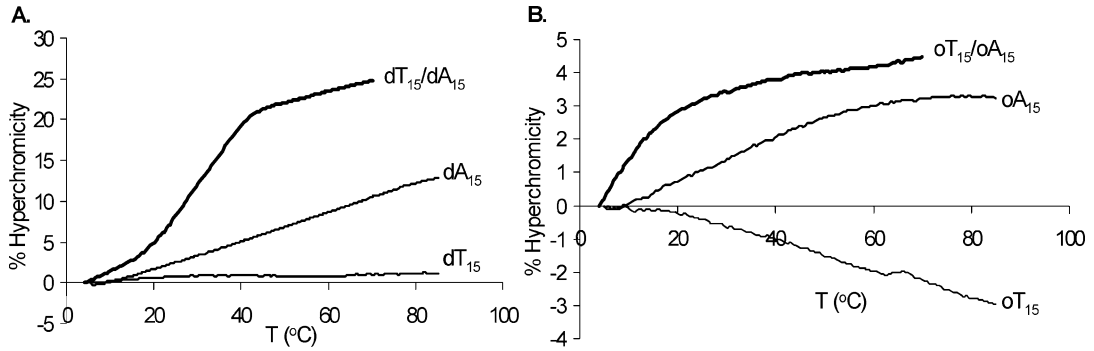

Figure 2. Comparison of T_m plots for (A) dT_{15}/dA_{15} and (B) oT_{15}/oA_{15} in addition to their single-stranded oligonucleotides. Duplex concentration was 3.04 μM in sodium phosphate buffer: 140 mM KCl, 1 mM $MgCl_2$, and 5 mM Na_2HPO_4 adjusted to pH = 7.

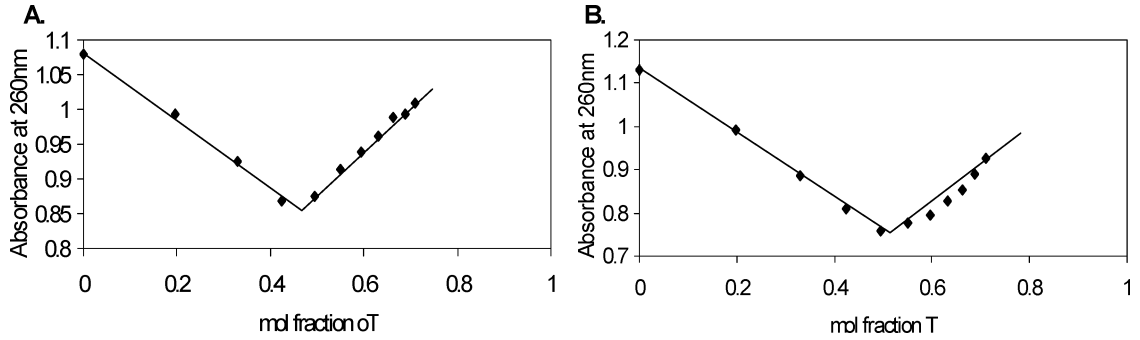

Figure 3. UV mixing curves at 5 °C for (A) oT_{15}/oA_{15} and (B) dT_{15}/dA_{15}. Concentration of each oligonucleotide stock solution was 5 μM, in duplex binding buffer: 10 mM Na_2HPO_4 and 100 mM NaCl, pH = 7.2.

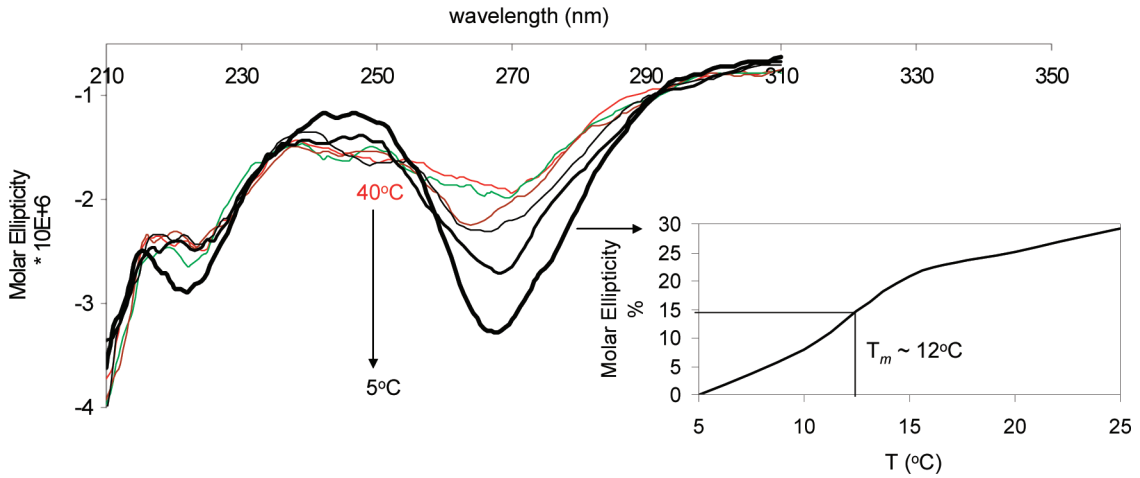

Figure 4. Temperature-dependent CD curves and representative plots for the change in molar ellipticity with temperature at λ_{max} 248 nm or λ_{min} 265 nm for oT_{15}/oA_{15}. (Inset)Percent change in molar ellipticity as a function of temperature at 265 nm and hybrid thermal denaturation curve. Concentration of duplex was 3.04 μM in sodium phosphate buffer: 140 mM KCl, 1 mM $MgCl_2$, and 5 mM Na_2HPO_4, pH = 7.

dA_{15}/dT_{15} (T_m = 37 °C) (Figure 2A; Table 2). Experiments with the individual strands alone showed, in the case of dA_{15} and oA_{15}, a slight increase in absorbance with temperature (Figure 2), consistent with a good stacking propensity observed for purine strands. This was not the case for oT_{15}, however, which displayed a decrease in absorbance with temperature (Figure 2B). Since the hyperchromicity change in the UV melting curve of oT_{15}/oA_{15} was small, more experiments were needed to evaluate whether the putative oT_{15}/oA_{15} duplex was formed. Data from the UV mixing (Job Plot)[34] studies were more conclusive, strongly suggesting that oT_{15} and oA_{15} base-pair into a helical complex with 1:1 stoichiometry at 5 °C (Figure 3A). The native dT_{15}/dA_{15} duplex also showed, as expected, UV mixing data consistent with a 1:1 complex (Figure 3B).

As another test for oT_{15}/oA_{15} complexation, we performed CD-monitored melting experiments (Figure 4). CD is particularly well suited for monitoring the melting of duplexes,[35] as single-phase transition from helix to coil state is often associated with the largest change in amplitude in the Cotton effect (molar ellipticity) at a given wavelength.[36] Samples were prepared as described above and the CD spectra were normalized against a blank solution containing the phosphate buffer. A parallel

(34) Pilch, D. S.; Levenson, C.; Shafer, R. H. *Proc. Natl. Acad. Sci. U.S.A.* **1990**, *87*, 1942−1946.
(35) Chan, S. S.; Breslauer, K. K.; Hogan, M. E.; Kessler, D. J.; Austin, R. H.; Ojemann, J.; Passner, J. M.; Wiles, N. C. *Biochemistry* **1990**, *29*, 6161−6171.
(36) Gray, D. M.; Hung, S.-H.; John, K. H. *Methods Enzymol.* **1995**, *246*, 19−34.

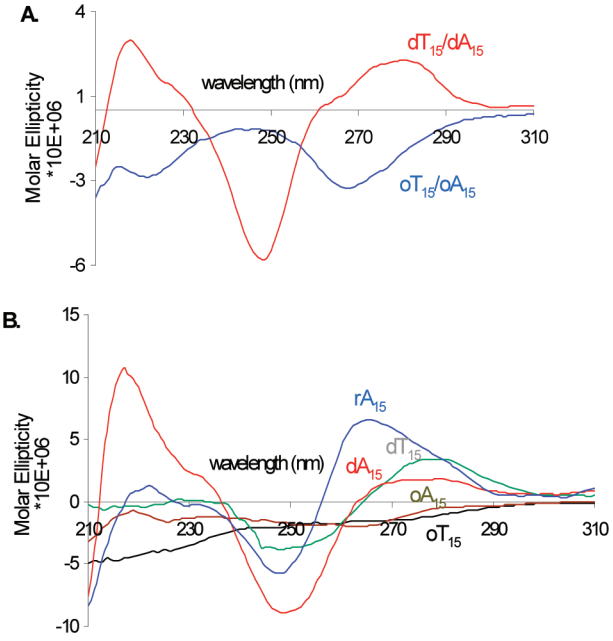

Figure 5. CD spectral signatures of the single-stranded and duplex oligonucleotides for (A) oT_{15}/oA_{15} and dT_{15}/dA_{15} duplexes and (B) oT_{15}, oA_{15}, dT_{15}, and dA_{15} single strands. Duplex concentration was 3.04 μM and single strand concentration was 1.52 μM in 140 mM KCl, 1 mM $MgCl_2$, and 5 mM Na_2HPO_4, pH = 7.

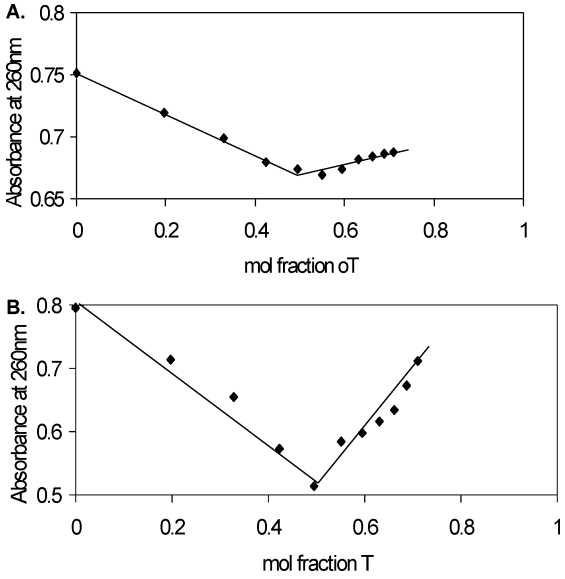

Figure 6. UV mixing curves at 5 °C for (A) oT_{15}/rA_{15} and (B) dT/rA_{15}. Concentration of each oligonucleotide stock solution was 5 μM in duplex binding buffer: 10 mM Na_2HPO_4 and 100 mM NaCl, pH = 7.2.

experiment was conducted with the native dT_{15}/dA_{15} duplex (see Supporting Information Figure S4) and the individual component strands (Figure 5B). The data obtained provided additional evidence for the interaction between oT_{15} and oA_{15}. Specifically, the CD spectra of the mixed oligomers oT_{15} and oA_{15} showed clear differences from those of the single strands (Figure 5), and a plot of the change in molar ellipticity as a function of temperature at 265 nm for oT_{15}/oA_{15} produced a sigmoidal hyperchromic transition from which a T_m value of ca. 12 °C was determined (Figure 4). This was in complete agreement with the T_m value obtained from UV melting measurements.

Of note, oT_{15}/oA_{15} exhibited a strikingly different CD profile from dT_{15}/dA_{15} (Figure 5A). The dT_{15}/dA_{15} hybrid exhibited the expected CD profile for a B-form helix, including a negative peak at 248 nm and a positive one at 278 nm.[37] By contrast, the oT_{15}/oA_{15} system displayed a nearly opposite signature that was characterized by negative minima at 265 and 220 nm and a negative maximum at 248 nm, suggesting the presence of a different helical form (Figure 5A). While the trace observed may be suggestive of a left-handed helix,[38] NMR and/or X-ray crystallographic studies will be required to conclusively establish the oT_{15}/oA_{15} duplex structure.[39]

2. Oxepane Nucleic Acid Cross-Pairs with RNA but Not Single-Stranded DNA. The single strands oT_{15} and oA_{15} were found to associate with their respective complementary RNA strands in 1:1 ratios to form oT_{15}/rA_{15} (T_m = 13 °C) and oA_{15}/rU_{15} (T_m = 12 °C) hybrids, respectively (Figure 6; Table 2 and Supporting Information Figure S3). These values were in agreement with the T_m values estimated from the temperature-dependent CD experiments (Figure 7 and Supporting Information Figure S7). The corresponding native hybrids dT_{15}/rA_{15} and dA_{15}/rU_{15} had melting temperatures of 32 and 16 °C, respectively (Table 2).[33,40]

No association (T_m < 5 °C) was detected between the oxepane oligomers and their complementary ssDNA strands (UV and CD thermal denaturation experiments). Consistent with this notion, the CD spectrum of oT_{15}/dA_{15} exhibited only a modest change in amplitude of the molar ellipticity with respect to the single strands, and the CD-monitored melting curve of the oT_{15} + dA_{15} mixture produced only a broad early transition of less than 5 °C (see Supporting Information Figure S8).

3. oT_{15}/rA_{15} and dT_{15}/rA_{15} Form an A-like Helix. The CD profiles of oT_{15}/rA_{15} and the native dT_{15}/rA_{15} systems are characteristic of A-like helices,[37] both displaying a strong positive band at 265 nm, a strong negative band near 248 nm, and a crossover point at around 254 nm. These similarities can be ascribed to the conformation of the underlying rA_{15} strand, which greatly influences the CD spectrum (Figure 8A). Given that the CD trace of the oT_{15} single strand alone (Figure 8B) is so different from that of rA_{15} and the oT_{15}/rA_{15} duplex, we conclude that oT_{15} readily adjusts to the dominant conformation of the purine RNA strand (rA_{15}). Compared to dT_{15} and rU_{15}, the oxepane oT_{15} single strand exhibited a unique spectral signature with small negative bands and no crossover points (Figure 8B). However, pairing between oT_{15} and rA_{15} provided a 1:1 complex at 5 °C (Figure 6) whose helical conformation very closely resembled that of the dT_{15}/rA_{15} hybrid (Figure 8A).

***Escherichia coli* RNase H-Mediated Degradation of oT/rA and pT/rA Hybrids.** The RNase H family comprises a class of enzymes that recognize and cleave the RNA strand of RNA−DNA heteroduplexes having topologies that are intermediate between the pure A- or B-form helices adopted by dsRNA and dsDNA, respectively.[41] Among the expanding list of sugar-modified ONs that elicit RNase H-mediated cleavage of RNA

(37) Steely, H. T.; Gray, D. M.; Ratliff, R. L. *Nucleic Acids Res.* **1986**, *14*, 10071−10090.
(38) (a) Wang, A. H.-J.; Quigley, G. J.; Kolpak, F. J.; Crawford, J. L.; van Boom, J. H.; van der Marel, G.; Rich, A. *Nature* **1979**, *282*, 680−686. (b) Nejedly, K.; Klysik, J.; Palecek, E. *FEBS Lett.* **1989**, *243* (2), 313−317. (c) Kagawa, T. F.; Howell, M. L.; Tseng, K.; Ho, P. S. *Nucleic Acids Res.* **1993**, *21* (25), 5978−5986.
(39) Tomasz, M.; Barton, J. K.; Magliozzo, C. C.; Tucker, D.; Lafer, E. M.; Stollar, B. D. *Proc. Natl. Acad. Sci. U.S.A.* **1983**, *80*, 2874−2878.
(40) Martin, F. H.; Tinoco, I. *Nucleic Acids Res.* **1980**, *8* (10), 2295−2299.

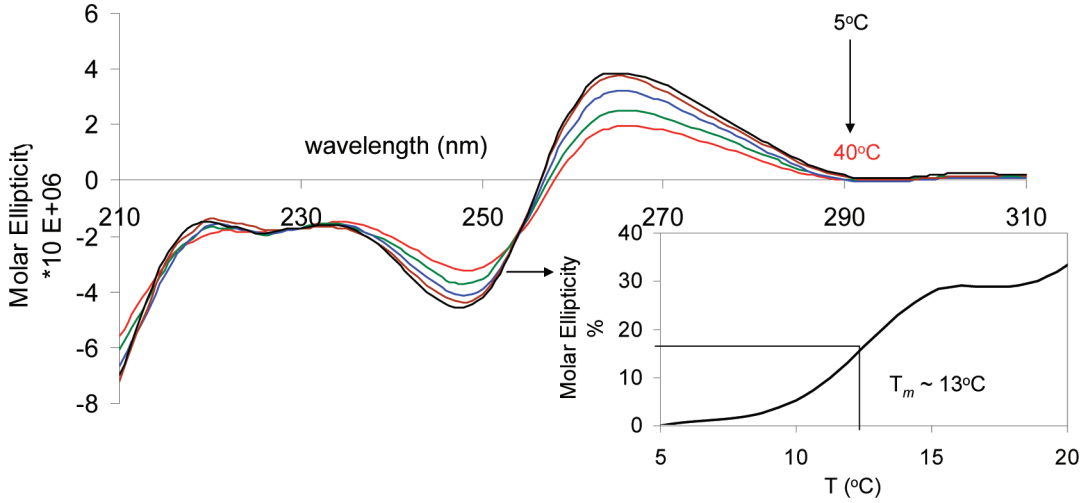

Figure 7. Temperature-dependent CD curves and representative plots for the change in molar ellipticity with temperature at λ_{min} 248 nm or λ_{max} 265 nm for oT_{15}/rA_{15}. (Inset) Percent change in molar ellipticity as a function of temperature at λ_{max} 265 nm and hybrid thermal denaturation curve. Concentration of duplex was 3.04 μM in sodium phosphate buffer: 140 mM KCl, 1 mM $MgCl_2$, and 5 mM Na_2HPO_4 pH = 7.

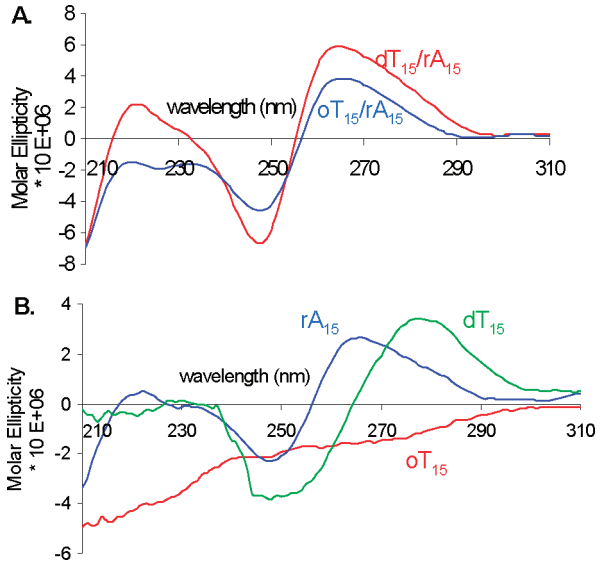

Figure 8. CD spectral signatures of single-stranded and duplex oligonucleotides for (A) oT_{15}/rA_{15} and dT_{15}/rA_{15} duplexes and (B) oT_{15}, rA_{15}, and dT_{15} single strands. Duplex concentration was 3.04 μM and single strand concentration was 1.52 μM in 140 mM KCl, 1 mM $MgCl_2$, and 5 mM Na_2HPO_4, pH = 7.

are arabino- (ANA) and 2′-deoxy-2′-fluoro-β-D-arabinonucleic acids (2′-F-ANA),[42] cyclohexene nucleic acids (CeNA),[8,16] and α-L-*ribo*-configured locked nucleic acids (α-L-LNA).[43] Chemical changes of the furanose or alterations in the orientation of the furanose to the base can dramatically diminish RNase H activation.[25,44] The discovery that 2′-*arabino*-configured locked bicyclonucleotide [3.3.0]bc-ANA satisfies the conformational requirements for RNase H recognition and cleavage without activating this enzyme suggests that the flexibility of the ON strand is critical as well.[45] A rigid ON seems to be unable to distort to allow its RNA complement to assume the conformation necessary for hydrolysis.[46,48]

The study of other carbohydrate systems, including non-furanose sugars, allows us to extend our understanding of the impact of backbone flexibility on RNase H activity.[6,7a,8,16] The insertion of a double bond in cyclohexane nucleic acids (i.e., cyclohexene NAs) is necessary for cross-pairing with RNA and activation of the RNase H enzyme.[8,16,47] To test whether the same effect operates in a pyranose system, we prepared a variant of the homo-DNA structure, the 2′-enopyranosyl modification (pT_{18}) previously reported by Felder et al.[21] The oligomer we prepared (pT_{18}) was capable of cross-pairing with the native rA_{18} complement strand (Table 1, $T_m \sim 25$ °C) and displayed a global helical conformation that resembled that of the native dT_{18}/rA_{18} substrate (see CD spectra, Supporting Information Figure S11). The oxepane and 2′-enopyranose backbones thus provide ring structures that are rendered more flexible than homo-DNA[13,14] and [3.3.0]bc-ANA[45] and conceivably are more likely to engage in interactions (i.e., H-bonding and base stacking) with the opposing RNA strand of the formed ON/RNA heteroduplex. This is demonstrated in Figure 9, which shows that both oT_{15}/rA_{15} and pT_{18}/rA_{18} support detectable cleavage by *E. coli* RNase H. Significantly less hydrolysis occurs for oT_{15}/rA_{15} when compared with the native substrate, which can be rationalized, at least in part, by the lower affinity of oT_{15} for the RNA target ($T_m \sim 13$ °C). This property acts to present a lower effective concentration of substrate duplex to the enzyme, thereby diminishing the overall rate of catalysis.

As we were interested in the relative rates of cleavage induced by the different ONs, this information was extracted from the assay conducted at 10 °C, at *a temperature that ensures the highest hybrid population for these systems* and under which enzyme activity is retarded just enough to enable a comparison

(41) (a) Uchiyama, Y.; Miura, Y.; Inoue, H.; Ohtsuka, E.; Ueno, Y.; Ikehara, M.; Iwai, S. *J. Mol. Biol.* **1994**, *243*, 782−791. (b) Nishizaki, T.; Iwai, S.; Ohtsuka, E.; Nakamura, H. *Biochemistry* **1997**, *36*, 2577−2585.
(42) (a) Damha, M. J.; Wilds, C. J.; Noronha, A.; Brukner, I.; Borkow, G.; Arion, D.; Parniak, M. A. *J. Am. Chem. Soc.* **1998**, *120*, 12976−12977. (b) Noronha, A. M.; Wilds, C. J.; Lok, C. N.; Viazovkina, K.; Arion, D.; Parniak, M. A.; Damha, M. J. *Biochemistry* **2000**, *39*, 7050−7062.
(43) Sorensen, M. D.; Kvaerno, L.; Bryld, T.; Hakansson, A. E.; Verbeure, B.; Gaubert, G.; Herdewijn, P.; Wengel, J. *J. Am. Chem. Soc.* **2002**, *124*, 2164−2176.
(44) Baker, B. F.; Monia, B. P. *Biochim. Biophys. Acta* **1999**, *1489*, 3−18.
(45) Nielsen, P.; Pfundheller, H. M.; Wengel, J. *Chem. Commun.* **1997**, 825−826.
(46) (a) Oda, Y.; Iwai, S.; Ohtsuka, E.; Ishikawa, M.; Ikehara, M.; Nakamura, H. *Nucleic Acids Res.* **1993**, *21*, 4690−4695. (b) Li, J.; Wartell, R. M. *Biochemistry* **1998**, *37*, 5154−5161.
(47) Maurinsh, Y.; Rosemeyer, H.; Esnouf, R.; Medvedovici, A.; Wang, J.; Ceulemans, G.; Lescrinier, E.; Hendrix, C.; Busson, R.; Sandra, P.; Seela, F.; Van Aerschot, A.; Herdewijn, P. *Chem.—Eur. J.* **1999**, *5* (7), 2139−2150.

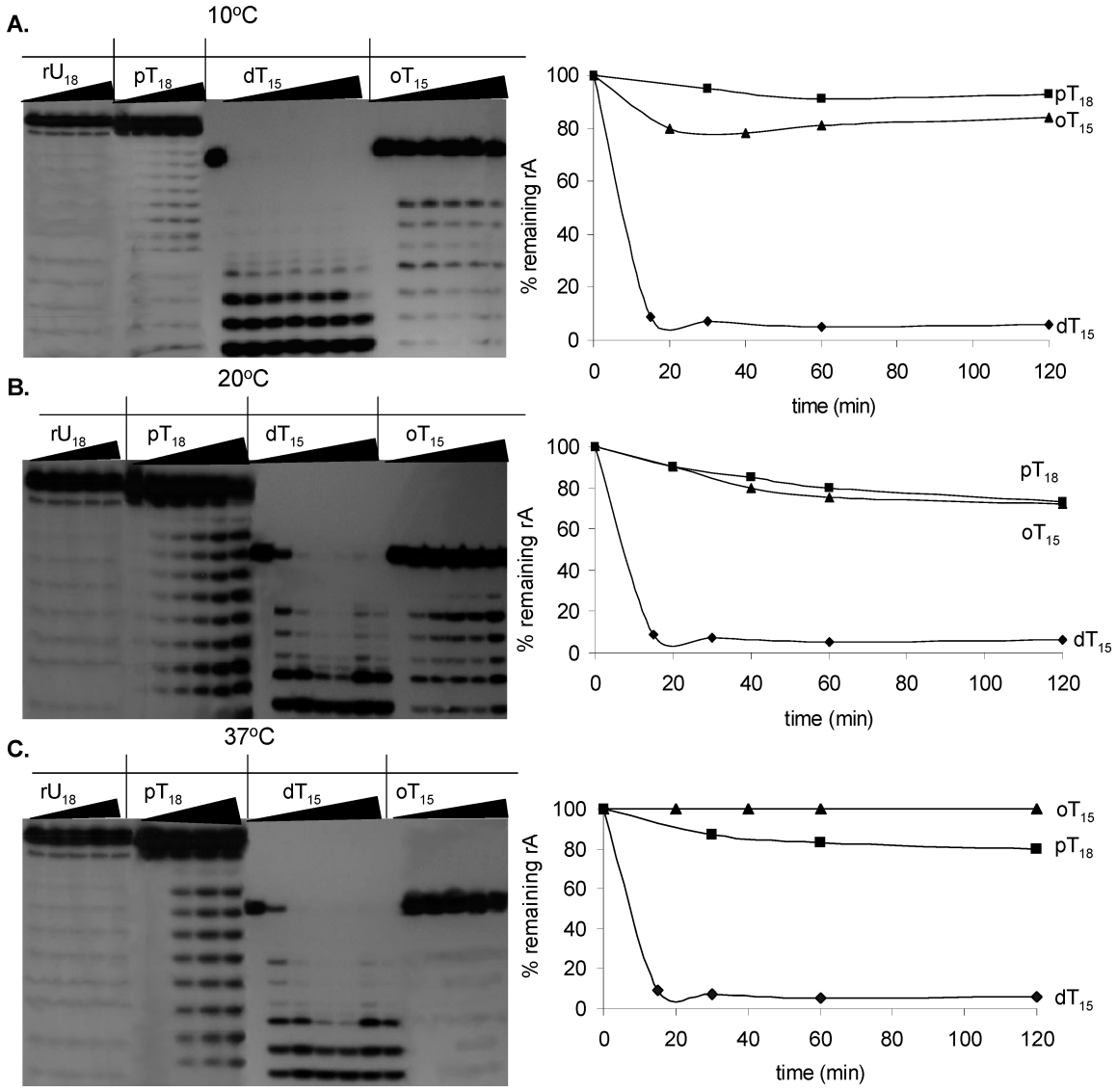

Figure 9. *E. coli* RNase H-mediated degradation of (A) 2′-OMe rU_{18}/rA_{18}, pT_{18}/rA_{18}, dT_{15}/rA_{15}, and oT_{15}/rA_{15} duplexes at 10 °C, for 0, 20, and 40 min and 1, 2, and 4 h; (B) 2′-OMe rU_{18}/rA_{18}, pT_{18}/rA_{18}, dT_{15}/rA_{15}, and oT_{15}/rA_{15} duplexes at 20 °C for 0, 10, 20, and 40 min and 1 and 2 h; (C) 2′-OMe rU_{18}/rA_{18}, pT_{18}/rA_{18}, dT_{15}/rA_{15}, and oT_{15}/rA_{15} duplexes at 37 °C for 0, 20, and 40 min and 1 and 2 h. The plots represent the hydrolysis profile of rA_{15} or rA_{18} as a function of temperature at 10, 20, and 37 °C for dT_{15}, pT_{18}, and oT_{15} complementary antisense strands.

of the extent of RNase H-mediated cleavage (Figure 9A). When we compared the relative rates of RNase H-mediated degradation induced by 5- (furanose, dT_{15}), 6- (2′-enopyranose, pT_{18}), and 7-membered (oxepane, oT_{15}) ring oligonucleotides *at 10 °C*, the following trends were observed: $dT_{15} \gg oT_{15} > pT_{18}$, which parallels the decreasing conformational flexibility of the constituent sugar rings, that is, furanose[10] (5) ≫ oxepane[11] (7) > 2′-enopyranose[12] (6). These results support the notion that the plasticity of the DNA/RNA hybrid is essential for efficient RNase H catalysis, in which an enzyme-induced altered trajectory of the bound substrate facilitates optimal interaction with RNase H's catalytic site.[6,7a,48]

Resistance of oT_{15} and oA_{15} toward Nuclease Degradation. Since resistance to exo- and endonucleases is imperative for in vivo applications of oligonucleotide-based therapeutics such as AONs, siRNAs, and aptamers,[49] we next determined the extent of nuclease resistance of oT_{15} and oA_{15} against 10% fetal bovine serum (FBS) at 37 °C. Under these conditions, the native dT_{15} and dA_{15} strands were degraded within 2 and 8 h, respectively, whereas the oxepane-modified oligomers (oT_{15} and oA_{15}) were completely resistant to cleavage under the same conditions with no noticeable degradation observed after 1 day (Supporting Information).

Conclusions

Replacement of the furanose carbohydrate with oxepane (oT_{15}) confers resistance to nucleases while retaining the ability to direct RNase H-mediated cleavage of a target RNA. The oT_{15} and pT_{18} oligomers of this study represent two new cases of chemically modified ONs capable of activating RNase H when bound to RNA, the others being, in chronological order, ANA,[42b] 2′-F-ANA,[42a] CeNA,[8,16] and α-L-LNA.[43] Although the extent to which cleavage occurs is lower than that observed for the

(48) Nielsen, J. T.; Stein, P. C.; Petersen, M. *Nucleic Acids Res.* **2003**, *31*, 5858−5867.

(49) Kandimalla, E. R.; Manning, A.; Zhao, Q.; Shaw, D. R.; Byrn, R. A.; Sasisekharan, V.; Agrawal, S. *Nucleic Acids Res.* **1997**, *25*(2), 370−378.

wild-type hybrid, it is significant that oT_{15} and pT_{18} are able to affect cleavage within the RNA component at all, in light of the dramatically different structure of their sugar moiety. This highlights the importance of sugar conformer flexibility along the ON strand, which likely acts in concert with the global helical architecture of the duplex to govern interactions between RNase H and its substrate. We are undertaking further studies with other ONA and 2′-enopyranose analogues obtained by functionalizing the double bond of nucleosides **2** and **13a**. These endeavors should afford further insight into the substrate requirements of the enzyme and provide a new repertoire of potent antisense and siRNA ONs.

Experimental Section

General. Thin-layer chromatography was performed with Merck Kieselgel 60 F-254 aluminum-back analytical silica gel sheets (0.2 mm thickness, EM Science, Gibbstown, NJ) and visualized with a solution of 10% H_2SO_4 in MeOH and/or UV light. ^{31}P NMR spectra were acquired on a Varian Gemini 200 MHz spectrometer at 80 MHz with ^1H decoupled and H_3PO_4 as external standard. Phosphoramidite samples were further characterized by ESI-MS on a Finnigan LCQ DUO mass spectrometer in methanol or acetone. UV spectra were measured at 260 nm on a Cary 300 dual-beam spectrophotometer.

3-Acetyl-1,5-anhydro-2-deoxy-1,2-*C*-methylene-4,6-*O*-(di-*tert*-butylsilanediyl)-D-glucal (1). Compound **1** was prepared according to slight modifications of the known literature procedure.[26,50] Commercially available tri-*O*-acetyl-D-glucal was used as starting material and initially deacetylated with 0.13 M NaOMe/MeOH for 1 h at room temperature. After evaporation of the solvent and concentration of the deprotected glycal as a white crystalline solid, the product was subsequently protected with di-*tert*-butylsilyldi(trimethylsilyl)trifluoromethanesulfonate, t-$Bu_2Si(OTf)_2$, in DMF at −40 °C to yield the 4,6-*O*-(di-*tert*-butylsilanediyl)-D-glucal after extraction and column chromatographic purification. The silylated glycal was subsequently subjected to cyclopropanation conditions according to Furukawa's modification[51] of the Simmons−Smith reaction with 1 M $ZnEt_2$ in hexanes and CH_2I_2. This reaction was followed by acetylation with Ac_2O in pyridine to yield the target compound **1**: ^1H NMR (**1**, $CDCl_3$, 400 MHz) δ 5.18 (1H, t, $J = 4.8$ Hz), 4.09 (1H, m), 4.09 (1H, dd, $J = 6.4$, 10 Hz), 3.69 (1H, t, $J = 6.8$ Hz), 3.65 (1H, t, $J = 6.4$ Hz), 3.42 (1H, m), 2.13 (3H, s), 1.58 (1H, m), 1.01 (9H, m), 0.98 (9H, m), 0.71 (2H, m); ^{13}C NMR (**1,** $CDCl_3$, 100 MHz, ^1H-decoupled at 400 MHz) δ 75.9, 75.1, 73.5, 66.2, 55.3, 27.95, 27.5, 23.23, 21.87, 16.7, 13.19; ESI-MS calcd for $C_{16}H_{28}O_5SiNa$ 342.5, found 343.3.

General Procedure for Glycosylation Reaction (2). The starting material **1** (4.7 mmol) was dried overnight under high vacuum. Similarly, in a separate flask, the base (thymine or N^6-benzoyladenine) (24 mmol) and drying agent $(NH_4)_2SO_4$ (2.5 mmol) were also dried under vacuum. Under a nitrogen atmosphere at 22 °C, 85 mL of dry MeCN was added to the flask containing the base and $(NH_4)_2SO_4$. Hexamethyldisilazane (HMDS, 38 mmol) was added dropwise to the resulting suspension, and the reaction was refluxed for 3−4 h until the MeCN-soluble silylated base was formed. The solvent was evaporated, a solution of **1** in 20 mL of dry MeCN was added and stirred at 22 °C under N_2, TMSOTf (1.6 mmol) was added dropwise, and the reaction was refluxed at 90 °C. The crude product was extracted with EtOAc (150 mL) followed by quenching and washing the upper organic layer with 100 mL each of saturated $NaHCO_3$ and H_2O. The upper organic layer was dried over $MgSO_4$ and evaporated to dryness, and the residue was purified on a column of silica gel [eluent 4:1 to 2:1 (v/v) hexanes/EtOAc].

(50) Oplinger, J. A.; Paquette, L. A. *J. Org. Chem.* **1998**, *53* (13), 2953−2959.
(51) (a) Furukawa, J.; Kawabata, N.; Nishimura, J. *Tetrahedron* **1968**, *24*, 53−58. (b) Hoveyda, A. H.; Evans, D. A.; Fu, G. C. *Chem. Rev.* **1993**, *93*, 1307−1370.

(1*R*)-1-[(2,3,4-Trideoxy-(5*S*,6*R*)-5,7-di-*tert*-butylsilanediyl)-β-oxepinyl]thymine (2a). The product **2a** was collected as its pure β-anomer as a white foam (650 mg, 35%): R_f (hexanes/EtOAc 2:1) 0.22; ^1H NMR ($CDCl_3$, 400 MHz) δ 8.56 (br s, NH), 7.19 (1H, d, $J = 1$ Hz, H6), 5.91 (1H, ddd, $J = 2.4$, 2.4, 12 Hz, H4′), 5.74 (1H, dd, $J = 6$, 10 Hz, H1′), 5.68 (1H, m, H3′), 4.59 (1H, dd, $J = 2.4$, 8.8 Hz, H5′), 4.06 (1H, dd, $J = 8.4$, 10.5 Hz, H7′), 3.85 (1H, dd, $J = 8.4$, 10.5 Hz, H7″), 3.64 (1H, m, H6′), 2.59 (1H, m, H2′), 2.39 (1H, m, H2″), 1.94 (3H, d, $J = 1$ Hz, H7), 1.05 (9H s, *t*-Bu Me), 0.99 (9H s, *t*-Bu Me); ^{13}C NMR ($CDCl_3$, 100 MHz, ^1H-decoupled at 400 MHz) δ 163.4 (CO), 149.8 (CO), 140 (C4′), 135.3, 122 (C3′), 111.36, 83.81 (C1′), 78.5 (C6′), 77 (C5′), 66.8 (C7′), 36.44 (*C*2′), 27.82 (*t*-Bu Me), 27.40 (*t*-Bu Me), 23.02 (*t*-Bu), 20.42 (*t*-Bu), 13.04; ESI-MS calcd for $C_{20}H_{32}O_5N_2Si$ 408.6, found 408.8.

Characterization of (1*R*)-1-[(2,3,4-Trideoxy-(5*S*,6*R*)-5,7-di-*tert*-butylsilanediyl)-β-oxepinyl]-N^6-benzoyladenine (2b). The product **2b** was collected as its pure β-anomer in yields of 710 mg (30%) as a white foam: R_f (EtOAc/hexanes 2:1) 0.24; ^1H NMR (acetone-d_6, 500 MHz) δ 10.0 (1NH, s, H6), 8.68 (1H, s, H8), 8.47 (1H, s, H2), 8−7.2 (5H, m, ar), 6.02 (1H, d, $J = 9$ Hz H1′), 5.90 (1H, dd, $J = 8$, 12 Hz, H3′), 5.76 (1H, dd, $J = 8.5$, 11 Hz, H4′), 4.74 (1H, d, $J = 9$ Hz, H5′), 4.04 (1H, ddd, $J = 14$, 10, 6 Hz, H7′), 3.91 (1H, dd, $J = 9.5$, 4.5 Hz, H6′), 3.86 (1H, d, $J = 18.5$ Hz, H7″), 3.40 (1H, d, $J = 14$ Hz, H2′), 2.84 (1H, m, H2″), 1.07 (9H, s, *t*-Bu Me), 1.04 (9H, s, *t*-Bu Me); ^{13}C (acetone-d_6, 125.7 MHz, ^1H−decoupled at 500 MHz) δ 152.16, 141.65, 139.3 (C3′), 132.6, 131.4, 128.75, 128.5, 128.4, 127.8, 127.6, 123.2 (C4′), 84.29 (C1′), 77.84 (C6′), 77.31 (C5′), 66.58 (C7′), 35.30 (C2′), 27.11 (*t*-Bu− Me), 26.78 (t-Bu− Me), 22.46 (*t*-Bu), 19.86 (*t*-Bu); ESI-MS calcd for $C_{27}H_{35}N_5O_4SiNa$ 544.7, found 544.1.

General Procedure for Desilylation Reaction. The starting material **2** (3.3 mmol) was dried overnight under vacuum. Under N_2 at 0 °C, the starting material was dissolved in 7 mL of THF. A solution of 1 M TBAF in dry THF (7 mL) was added with stirring over 5 min. The reaction mixture turned slightly cloudy as the deprotected nucleoside slowly began to precipitate from the solvent. The reaction was complete by TLC after 1 h, so the solvent was removed and the resulting viscous oil was purified by column chromatography (9:1 CH_2Cl_2/MeOH) to give a white foam.

(1*R*)-1-[(2,3,4-Trideoxy-(5*S*,6*R*)-5-hydroxy-7-hydroxymethyl)-β-oxepinyl]thymine (4). Yield 0.854 g (90%); R_f (9:1 CH_2Cl_2/MeOH) 0.37; ^1H NMR (DMSO-d_6, 500 MHz) δ 11.30 (1NH, s, H3), 7.57 (1H, s, H6), 5.74 (1H, t, $J = 9$ Hz, H4′), 5.60 (1H, d, $J = 10$ Hz, H1′), 5.55 (1H, d, $J = 9$ Hz, H3′), 4.05 (1H, d, $J = 7.5$ Hz, H5′), 3.60 (1H, d, J= 11 Hz, H7′), 3.46 (1H, d, $J = 11$ Hz, H7″), 3.36 (1H, t, $J = 6.5$ Hz, H6′), 3.14 (d, OH), 2.67 (1H, t, $J = 12$ Hz, H2′), 2.32 (1H, dd, $J = 6$, 7.5 Hz, H2″), 1.76 (3H, s, 7), 1.55 (s, OH); ^{13}C NMR (DMSO-d_6, 125 MHz, ^1H-decoupled at 500 MHz) δ 164.22 (CO), 150.33 (CO), 138.03 (C3′), 136.31 (C6), 83.45 (C1′), 34.89 (C2′), 122.27 (C4′), 68.91 (C5′), 84.80 (C6′), 61.95 (C7′), 23.06 (C7), 108.93 (C5); ESI-MS calcd for $C_{12}H_{16}N_2O_5$ 268.7, found 269.

(1*R*)-1-[(2,3,4-Trideoxy-(5*S*,6*R*)-5-hydroxy-7-hydroxymethyl)-β-oxepinyl]-N^6-benzoyladenine (5). Yield 184 mg (61%); R_f [9:1 (v/v) CH_2Cl_2/MeOH] 0.33; ^1H NMR (MeOH-d_4, 500 MHz) δ 8.71 (1H, s, H8), 8.58 (1H, s, H2), 8.08 (2H, d, ar), 7.65 (1H, m, ar), 7.56 (2H, m, ar), 6.09 (1H, dd, $J = 9.5$, 2.5 Hz, H1′), 5.92 (ddd, 1H, $J = 2.5$, 13 Hz, H3′), 5.76 (1H, m, H4′), 4.28 (1H, dd, $J = 2$, 9 Hz, H5′), 3.89 (1H, dd, $J = 4.5$, 9.5 Hz, H7′), 3.79 (1H, ddd, $J = 2.5$, 5, 9 Hz, H6′), 3.68 (1H, dd, $J = 6$, 11.5 Hz, H7″), 3.17 (1H, m, H2′), 3.05 (OH), 2.90 (1H, ddd, $J = 2$, 7, 16.5 Hz, H2″), 1.65 (OH); ^{13}C NMR (MeOH-d_4, 125.7 MHz, ^1H-decoupled at 500 MHz) δ 175.23 (CO), 152.0 (C8), 142.2 (*C*2), 137.6 (C3′), 132.7 (ar), 128.6 (ar), 128.2 (ar), 122.3 (C4′), 84.90 (C1′), 84.29 (C6′), 69.92 (C5′), 62.83 (C7′), 35.23 (C2′); ESI-MS calcd for $C_{19}H_{19}N_5O_4$ 402.6, found 404.

General Procedure for Hydrogenation Reaction. The product from the desilylation reaction (0.565 mmol) and 152 mg of 10% Pd/C catalyst were dried overnight under vacuum. Dry MeOH (11.5 mL) was added

to the evacuated flask and the dark suspension was stirred at room temperature (22 °C). A balloon filled with H_2 was attached to the flask by piercing the septum with a needle. Small aliquots were periodically withdrawn and evaporated to dryness, and the extent of reaction was verified by ^{1}H NMR. After 4 h, the remaining reaction mixture was filtered and evaporated to dryness. The crude product was purified by flash silica gel column chromatography in 9:1 CH_2Cl_2/MeOH.

(1*R*)-1-[(2,3,4-Trideoxy-(5*S*,6*R*)-5-hydroxy-7-hydroxymethyl)-*β*-oxepanyl]thymine (6). The extent of reaction could not be accurately monitored by TLC, as the R_f values for the starting material and product were found to be identical in eluent system 9:1 CH_2Cl_2/MeOH. The product was obtained in 70% yield (104 mg) as a white foam after silica gel column chromatography (9:1 CH_2Cl_2/MeOH): R_f (9:1 CH_2Cl_2/MeOH) 0.21; ^{1}H NMR (MeOH-d_4, 500 MHz) δ 7.56 (1H, s, H6), 5.78 (1H, d, J = 9.5 Hz, H1′), 3.77 (1H, s, H5′), 3.70 (1H, d, J = 11.5 Hz, H7′), 3.55 (1H, m, H6′), 3.55 (1H, m, H7″), 1.97 (1H, m, H2′), 1.90 (2H, m, H3′, H3″), 1.90 (3H, s, H7), 1.88 (2H, m, H4′, H4″), 1.66 (1H, d, J = 6 Hz, H2″); ^{13}C NMR (MeOH-d_4, 125 MHz, ^{1}H−decoupled at 500 MHz) δ 150.9 (CO), 137 (C6), 110 (CO), 95 (C5), 86.64 (C6′), 86.5 (C1′), 70.8 (C5′), 63.37 (C7′), 34.87 (C4′), 33.29 (C3′), 17.9 (C2′) 11.18 (C7); ESI-MS calcd for $C_{12}H_{18}N_2O_5Na$ 279.3, found 293.1.

(1*R*)-1-[(2,3,4-Trideoxy-(5*S*,6*R*)-5-hydroxy-7-hydroxymethyl)-*β*-oxepanyl]-*N*^{6}-benzoyladenine (7). Compound **7** was isolated in 99% yield (149 mg) as a white foam after silica gel column chromatography (9:1 CH_2Cl_2/MeOH): R_f (9:1 CH_2Cl_2/MeOH) 0.22; ^{1}H NMR (MeOH-d_4, 500 MHz) δ 9.81 (1NH, s), 8.71 (1H, s, H8), 8.58 (1H, s, H2), 8.08 (2H, ar), 7.65 (1H, ar), 7.56 (2H, ar), 6.06 (1H, dd, J = 5, 5.5 Hz, H1′), 3.80 (1H, dd, J = 4, 8.25 Hz, H6′), 3.76 (1H, dd, J = 3, 6 Hz, H4′), 3.58 (1H, dd, J = 6.35, 12 Hz, H4″), 3.12 (1H, t, J = 8 Hz, H5′), 2.39 (2H, m, H2′, H2″), 2.04 (2H, m, H3′, H3″), 1.93(1H, m, H7′), 1.81 (1H, m, H7″), 1.67 (OH), 1.42 (OH); ^{13}C NMR (MeOH-d_4, 125.7 MHz, ^{1}H-decoupled at 500 MHz) δ 151.9 (C8), 142 (C2), 132.7 (ar), 128.6 (ar), 128.3 (ar), 87.25 (C1′) 70.68 (C5′), 63.54 (C4′), 52.90 (C6′), 35.08 (C2′), 33.76 (C3′), 18.0 (C7′); ESI-MS calcd for $C_{19}H_{21}N_5O_4Na$ 406.4, found 406.4.

General Procedure for Tritylation Reaction. Nucleoside **6** or **7** (0.377 mmol) and MMT−Cl (0.44 mmol), were dried overnight under vacuum. Pyridine (1.5 mL) was added at 22 °C under nitrogen. The reaction was stirred for 4 h until TLC (9:1 CH_2Cl_2/MeOH) indicated completion. The reaction was diluted with EtOAc (60 mL) and washed with saturated aqueous $NaHCO_3$ (2 × 60 mL). The organic layer was then dried over $MgSO_4$, concentrated, and purified by silica gel chromatography (9:1 CH_2Cl_2/MeOH).

(1*R*)-1-[(2,3,4-Trideoxy-(5*S*,6*R*)-5-hydroxy-7-[4-(methoxyphenyl)-diphenyl])-*β*-oxepanyl]thymine (8). Yield 66% (135 mg) as a white foam; R_f (9:1 CH_2Cl_2/MeOH) 0.68; ^{1}H NMR ($CDCl_3$, 500 MHz) δ 8.85 (1H, s, NH), 7.34 (4H, ar), 7.2 (1H, s, H6),. 7.19 (8H, ar), 6.76 (2H, ar), 5.74 (1H, dd, J = 3.6, 9.8 Hz, H1′), 3.83 (H1, ddd, J = 3.6, 4.8, 7.6 Hz, H5′), 3.72 (s, OMe), 3.6 (1H, dd, J = 6, 12.6 Hz, H6′), 3.31 (1H, dd, J = 5.6, 9.6 Hz, H7), 3.11 (1H, dd, J = 5.6, 9.6 Hz, H7″), 1.98 (1H, dd, J = 3.6, 9 Hz, H3′), 1.78 (1H, m, H3″), 1.80 (2H, m, H4′, H4″), 1.86 (3H, d, J = 1 Hz, H7), 1.62 (2H, dd, J = 8.4, 14.4 Hz, H2′, H2″); ^{13}C ($CDCl_3$, 125.7 MHz, ^{1}H-decoupled at 500 MHz) δ 163.79 (CO), 158.93 (CO), 149, 144.3,144,1, 135.9 (C6), 135.2, 130.6, 128.5, 128.2, 127.3, 113.5, 110.9, 86.53 (C1′), 87.16 (C5), 83.58 (C6′), 73.41 (C5′), 65.90 (C7′), 55.47 (OMe), 35.81 (C3′), 33.48 (C4′), 18.31 (C2′), 12.86 (C7); ESI-MS calcd for $C_{32}H_{34}N_2O_6Na$ 565.6, found 565.1.

(1*R*)-1-[(2,3,4-Trideoxy-(5*S*,6*R*)-5-hydroxy-7-[4-(methoxyphenyl)-diphenyl])-*β*-oxepanyl]-*N*^{6}-benzoyladenine (9). Yield 50% (120 mg) as a white foam; R_f (9:1 CH_2Cl_2/MeOH) 0.65; ^{1}H ($CDCl_3$, 500 MHz) δ 9.03 (1H, s, H4), 8.14 (1H, s, H2), 8.72 (1H, s, H8), 7.95 (2H, ar), 7.52 (1H, ar), 7.44 (2H, ar), 7.29 (3H, ar), 7.17 (8H, ar), 6.71 (2H, ar), 5.99 (1H, dd, J = 2.8, 10 Hz, H1′), 3.90 (1H, t, J = 8.4 Hz, H6′), 3.79 (1H, dd, J = 5.6, 12.6 Hz, H5′), 3.71 (OMe), 3.30 (1H, dd, J = 5.6, 9.6 Hz, H4′), 3.14 (1H, dd, J = 6, 9.6 Hz, H4″), 2.27 (1H, ddd, J = 3, 6.5, 15.6 Hz, H2′), 2.16 (1H, ddd, J = 4.8, 9, 15.6 Hz, H2″), 1.99 (1H, dd, J = 4.8, 17.2 Hz, H3′), 1.92 (1H, dd, J = 2.8, 17.2 Hz, H3″), 1.82 (1H, ddd, J = 4, 8.4, 16 Hz, H7′), 1.73 (1H, t, J = 8.4 Hz, H7″); ^{13}C ($CDCl_3$, 125.7 MHz, ^{1}H-decoupled at 500 MHz) δ 158.9 (CO), 152.8 (C8), 144.3, 140.6 (C2), 144.1, 135.2, 132.98, 130.5, 129.5, 129.1, 128.48, 128.13, 128.1, 128.08, 127.4, 127.3, 113.5, 95, 87.2, 86.44 (C1′), 83.71 (C5′), 73.28 (C6′), 65.88 (C4′), 55.44 (OMe), 36.08 (C2′), 33.61 (C7′), 18.37 (C3′); ESI-MS calcd for $C_{39}H_{37}N_5O_5$ 655.9, found 655.7.

General Procedure for Phosphitylation Reaction. The tritylated nucleoside (0.224 mmol) was dried under vacuum overnight prior to reaction. Dry THF (1.2 mL) was added under N_2. To the resulting solution were added dropwise, over a span of 10 min, EtN(*i*-Pr)$_2$ (0.89 mmol) and Cl$^-$-P(OCEt)N(*i*-Pr)$_2$ (0.246 mmol). The reaction mixture was stirred for 2 h at 22 °C, and the reaction progress was monitored by TLC (hexanes/EtOAc 2:1). The progression of the reaction is also observable by the formation of a white precipitate, Cl^{-+}NH(Et)(*i*-Pr)$_2$. After the reaction reached completion, EtOAc (15 mL) was added and the mixture was washed twice with saturated aqueous $NaHCO_3$, dried over $MgSO_4$, and concentrated to a yellowish foam, which was purified by silica gel chromatography (hexanes/EtOAc 2:1 to 1:2 containing 3% TEA).

(1*R*)-1-[(2,3,4-Trideoxy-(5*S*,6*R*)-5-phosphoramidous-7-[4-(methoxyphenyl)diphenyl])-*β*-oxepanyl]thymine (10). Yield 131 mg (80%) as a white foam; R_f (2:1 hexanes/EtOAc) 0.52; ^{31}P NMR ($CDCl_3$, 80.99 MHz, ^{1}H-decoupled at 200 MHz) δ 149.5 and 149.02; ESI-MS calcd for $C_{41}H_{51}N_4O_7PNa$ 765.86, found 765.2.

(1*R*)-1-[(2,3,4-Trideoxy-(5*S*,6*R*)-5-phosphoramidous-7-[4-(methoxyphenyl)diphenyl])oxepanyl]-*N*^{6}-benzoyladenine (11). Yield 135 mg (92%) as white foam; R_f (2:1 hexanes/EtOAc) 0.33; ^{31}P NMR ($CDCl_3$, 80.99 MHz, ^{1}H-decoupled at 200 MHz) δ 148.4 and 147.9; ESI-MS calcd for $C_{48}H_{54}N_7O_6PNa$ 878.9, found 878.3.

1-(2,3-Dideoxy-4,6-di-*O*-acetyl-D-*erythro*-hex-2-enopyranosyl)thymine α- and *β*-Anomers (13). The starting material **12** (7.35 mmol) was dried separately from thymine (14.7 mmol) and the drying agent $(NH_4)_2SO_4$ (1.4 mmol) overnight under high vacuum. Anhydrous MeCN (56 mL) under N_2 at 22 °C was added to the reaction flask containing thymine and the drying agent, and the mixture was stirred to a white slurry suspension prior to dropwise addition of HMDS (23.85 mmol) to initiate the silylation reaction of the base. The reaction was refluxed to completion at 100 °C for 3−4 h and the solvent was evaporated to a viscous yellowish oil. A solution of the starting material **12** in 30 mL of anhydrous MeCN was stirred at 22 °C under N_2 and transferred to the silylated thymine. The coupling reaction was initiated after dropwise addition of TMSOTf (11 mmol) and completed for 3 h under reflux at 90 °C as was monitored by TLC: R_f (2:1 hexanes/EtOAc) = 0.29 and 0.20 for the *β*- and α-anomers, respectively. The crude reaction mixture was diluted with EtOAc (200 mL) and in turn quenched and washed with $NaHCO_3$ and H_2O (150 mL). The organic layer was dried over $MgSO_4$ and concentrated for chromatographic purification with eluent gradient of 4:1 hexanes/EtOAc to 2:1 EtOAc/hexanes. The purified *β*-anomer, **13a**, was collected with a yield of 765 mg (35%) and the α-anomer, **13b**, was collected with a yield of 935 mg (40%).

1-(2,3-Dideoxy-4,6-di-*O*-acetyl-*β*-D-*erythro*-hex-2-enopyranosyl)-thymine (13a). ^{1}H NMR ($CDCl_3$, 400 MHz) δ 8.16 (s, NH), 6.96 (1H, s, H5), 6.52 (1H, s, H1′), 6.16 (1H, d, H3′), 5.75 (1H, d, J = 10 Hz, H2′), 5.38 (1H, d, J = 6.5 Hz, H4′), 4.20 (2H, d, J = 3.5 Hz, H6′, H6″), 4.00 (1H, t, J = 4.5 Hz, H5′), 2.11 (3H, s, OAc), 2.08 (3H, s, OAc), 1.91 (3H, s); ^{13}C NMR ($CDCl_3$ 125.7 MHz, ^{1}H-decoupled at 500 MHz) δ 169.3 (CO), 168.8 (CO), 161.7 (CO), 148.8 (CO), 131.2 (C3′), 134.1 (C6), 126.3 (C2′), 110.77 (C5), 77.19 (C1′), 73.77 (C5′), 62.89 (C4′), 61.53 (C6′), 19.83 (OAc), 19.73 (OAc), 11.42 (C7); ESI-MS calcd for $C_{15}H_{18}N_2O_7$ 338.9, found 338.3.

1-(2,3-Dideoxy-4,6-di-*O*-acetyl-α-D-*erythro*-hex-2-enopyranosyl)-thymine (13b). ^{1}H NMR ($CDCl_3$, 400 MHz) δ 8.18 (s, NH), 7.24 (1H, s, H5), 6.40 (1H, s, H1′), 6.30 (1H, d, J = 10 Hz, H3′), 5.86 (1H, d,

J = 10.5 Hz, H2′), 5.24 (1H, d, J = 3 Hz, H4′), 4.27 (1H, dd, J = 12 Hz, H6′), 4.16 (1H, dd, J = 3, 12.25 Hz, H6″), 4.01 (1H, m, J = 4.5 Hz, H5′), 2.12 (s, OAc), 2.09 (s, OAc), 1.93 (3H, s, H7); ESI-MS calcd for $C_{15}H_{18}N_2O_7$ 338.9, found 338.3.

1-(2,3-Dideoxy-β-D-*erythro*-hex-2-enopyranosyl)thymine (14). The starting material, **13a** (2.07 mmol), was vacuum-dried overnight prior to reaction. Under N_2 and at 22 °C, the starting material was dissolved in 10 mL of anhydrous MeOH followed by dropwise addition of a 0.1 M NaOMe/MeOH (7 mL) solution. The reaction proceeded for 1 h, and the product was confirmed by TLC [R_f (9:1 CH_2Cl_2/MeOH) = 0.2]. The crude reaction mixture was concentrated to a white slurry and purified by column chromatography with eluent system 9:1 CH_2Cl_2/MeOH. The purified product was collected as a white foam, yield 0.485 g (93%); ^{1}H NMR (DMSO-d_6, 400 MHz) δ 11.34 (s, NH), 7.16 (1H, s, H6), 6.23 (1H, s, H1′), 6.08 (1H, d, J = 11 Hz, 3′), 5.64 (1H, d, J = 10.4 Hz, H2′), 5.27 (s, OH), 4.71 (s, OH), 4.03 (1H, d, J = 6.8 Hz, H4′), 3.67 (1H, d, J = 11 Hz, H6′), 3.46 (1H, m, H6″), 3.30 (1H, s, H5′), 1.76 (1H, s, H7); ^{13}C NMR (DMSO-d_6, 125.7 MHz, ^{1}H-decoupled at 500 MHz) δ 163.8 (CO), 150.5 (CO), 137.3 (C3′), 136.5 (C6), 124.9 (C2′), 109.9 (C5), 81.06 (C5′), 77.99 (C1′), 61.24 (C4′), 60 (C6′), 11.99 (C7); ESI-MS calcd for $C_{11}H_{14}N_2O_5$ 254.3, found 254.2.

1−{(4*S*,5*R*)-4-Hydroxy-6-[4-(methoxyphenyl)diphenyl]-2,3-dideoxy-β-D-*erythro*-hex-2-enopyranosyl}thymine (15). The starting material, **14** (1.91 mmol), and MMT−-Cl (2.20 mmol) were dried under high vacuum prior to the start of the reaction. The reaction was initiated at 22 °C under N_2 by dropwise addition of anhydrous pyridine (8 mL) and stirred to complete reaction for 3 h, as was monitored by TLC [R_f (9:1 CH_2Cl_2/MeOH) = 0.68]. The crude reaction mixture was diluted in 35 mL of EtOAc or Et_2O and quenched with $NaHCO_3$ (2 × 20 mL) prior to being dried over $MgSO_4$ and evaporated to dryness. The crude reaction mixture was purified by silica gel chromatography, with eluent gradient ranging from 151 to 9:1 CH_2Cl_2/MeOH. The product was collected as a white foam, 0.78 mg (78% yield); ^{1}H NMR ($CDCl_3$, 400 MHz) δ 8.61 (NH), 7.40, 7.27, 6.84, (MMT), 6.94 (1H, d, J = 2 Hz, H6), 6.42 (1H, d, J = 2 Hz, H1′), 6.20 (1H, ddd, J = 2, 10 Hz, H3′), 5.64 (1H, ddd, J = 1.8, 3.6, 10 Hz, H2′), 4.30 (1H, dd, J = 2.4, 8.4 Hz, H4′), 3.82 (OCH_3), 3.80 (1H, m, H5′), 3.58 (1H, dd, J = 4.8, 9.2 Hz, H6′), 3.31 (1H, dd, J = 6.4, 9.2 Hz, H6″), 1.90 (1H, d, H5); ^{13}C NMR ($CDCl_3$, 100 MHz, ^{1}H-decoupled at 400 MHz) δ 163.4 (CO), 158.8 (CO), 150.4, 149.1, 143.6, 136.3 (C2′), 135.89 (C6), 134.7, 130.4, 128.3, 128.2, 127.9, 127.4 (C3′), 125.4, 123.96 (C7′), 111.7(C5), 87.8, 78.64 (C1′), 77.64 (C5′), 66.3 (C4′), 65.5 (C6′), 55.6 (OMe), 13.01; ESI MS calcd for $C_{31}H_{30}N_2O_6$ 549.4, found 549.1.

1-[(2,3-Dideoxy-(4*S*,5*R*)-5-[4-(methoxyphenyl)diphenyl]-4-phosphoramidous-β-D-*erythro*-hex-2-enopyranosyl)thymine (16). The starting material, **15** (1.48 mmol), was vacuum-dried overnight prior to the start of the reaction. At 22 °C and under N_2, the starting material was dissolved in anhydrous THF (8 mL) and the reaction was initiated by dropwise addition of EtN(*i*-Pr)$_2$ (5.6 mmol) and Cl$^-$-P(OCEt)N(*i*-Pr)$_2$ (1.56 mmol). The reaction was monitored to completion by TLC [R_f (2:1 EtOAc/hexanes) = 0.59]. The crude reaction mixture was diluted in EtOAc or Et_2O (70 mL) and quenched/washed with saturated $NaHCO_3$ (2 × 30 mL). The upper organic layer was dried over $MgSO_4$ and evaporated to a yellow-tinged foam. The product was then purified by column chromatography with eluent gradient of 2:1 hexanes/EtOAc to 2:1 EtOAc/hexanes with 3% TEA. The purified phosphoramidite diastereomers were collected with a yield of 825 mg (80%) as a white foam: ^{31}P NMR ($CDCl_3$, 80 MHz, ^{1}H-decoupled at 200 MHz) δ 151.8 and 150.1; ESI-MS calcd for $C_{40}H_{47}N_4O_7PNa$ 749.8, found 749.2.

Oligonucleotide Synthesis. Synthesis of modified oligonucleotides was performed on a 500 Å Unylinker CPG on a 0.5−1 μmol scale. Phosphoramidites were prepared as 0.05−0.1 M solutions (**10** in CH_2Cl_2, **11** and **16** in MeCN). The coupling times were 30 min with 0.25 M ETT in MeCN as activator. The detritylation time was extended to 2.5 min. Oligonucleotides were cleaved from the CPG and base-protecting groups were removed by overnight incubation at 55 °C in saturated NH_4OH/EtOH (3:1). The deprotected oligonucleotides were evaporated to dryness, extracted from the CPG with 1 mL of sterile H_2O, and quantitated by UV/vis spectrophotometry. Crude ONA oligonucleotides were purified by denaturing PAGE or anion-exchange HPLC with a 30% gradient of 1 M $LiClO_4$. Purified oligonucleotides were extracted and desalted with Nap 10 Sephadex columns.

Characterization of Oligonucleotides by MALDI-TOF Mass Spectrometry. All spectra were acquired on a Kratos Kompact-III instrument operated in the negative linear mode for 200 pmol of oligonucleotide sample dissolved in 1 μL of H_2O, 1 μL of 6-aza-2-thiothymine/spermine, and 1 μL of 50 mM aqueous L-fucose mixture.

UV Thermal Denaturation Experiments, T_m. The studies were conducted on a UV−vis Cary 300 dual-beam spectrophotometer for 3 μM duplex in a phosphate buffer that mimics the physiological ionic strength: 140 mM KCl, 5 mM NaH_2PO_4, and 1 mM $MgCl_2$, pH = 7. The solutions were denatured at 85 °C for 10 min and then cooled to room temperature over 2.5 h and kept at 5 °C overnight prior to the experiment. The thermal melt measurements were run from 5 −to 85 °C with temperature gradient increases of 0.5 °C/min and data point intervals of 0.5/min at a wavelength of 265 nm.

CD Experiments. Duplexes were prepared as for UV T_m analysis. Samples were analyzed on a Jasco Model J-710 or J-810 spectropolarimeter with temperature controlled with a circulating bath (VWR Scientific) in the 310−210 nm wavelength range as the sum of three replicates which were finally baseline-corrected from the phosphate buffer used (140 mM KCl, 5 mM NaH_2PO_4, and 1 mM $MgCl_2$, pH = 7). For the temperature-dependent CD-melt experiments, the samples were allowed to equilibrate for 5−10 min under N_2 at a fixed temperature prior to the runs.

UV Mixing Curves. The studies were conducted on a UV−vis Cary 300 dual beam spectrophotometer. Equimolar stock solutions of each oligonucleotide (2.5 nmol) were prepared in 0.5 mL of buffer (10 mM Na_2HPO_4 and 100 mM NaCl, pH = 7.2). At low temperature (5 °C), 100 μL aliquots (0.5 nmol) of T solution were titrated into the stock solution containing A and allowed to hybridize for 5−10 min prior to measuring the UV absorbance at 260 nm under constant flow of N_2. Absorbance values were measured at 260 nm for each mol fraction of T titrated into a fixed concentration of complementary A stock solution.

Serum Stability of Oligonucleotides. Pure oligothymidylate and oligoadenylate (0.7 OD) were evaporated to dryness. To each dried oligonucleotide sample was added 300 μL of 10% FBS (0.2 μM, in 10% fetal bovine serum diluted with Eagle's medium) and incubated at 37 °C for up to 24 h. For each time point, a 50 μL aliquot of the reaction mixture was removed and frozen on dry ice for 10 min followed by evaporation in a SpeedVac concentrator. Aliquots were redissolved in deionized formamide and analyzed by denaturing 24% PAGE, visualized by Stains-All dye.

RNase H Assays. The RNA strand (200 pmol) was initially 5′-radiolabeled with T4 polynucleotide kinase and [γ-^{32}P]ATP. A 1.8-fold excess of 15- or 18-mer oligothymidylate was added to the purified RNA strand and annealed in 100 μL solutions containing 0.5× reaction buffer (i.e., 20 pmol in 10 μL of buffer; 100 mM Tris−HCl, pH = 7.5, 100 mM KCl, 50 mM $MgCl_2$, 0.5 mM EDTA, and 0.5 mM DTT). *E. coli* RNase H assays were performed at different temperature conditions (10, 20, and 37 °C) in 10 μL reactions containing 2 pmol of duplex substrate with 2 μL of reaction buffer (100 mM Tris−HCl, pH = 7.5, 100 mM KCl, 50 mM $MgCl_2$, 0.5 mM EDTA, and 0.5 mM DTT) and 0.5 μL of *E. coli* RNase H enzyme (concentration 5 units/μL in storage buffer: 20 mM Tris−HCl, pH = 7.9, 100 mM KCl, 10 mM $MgCl_2$, 0.1 mM EDTA, 0.1 mM DTT, and 50% glycerol). Each reaction was quenched at various time points by heating to 90 °C and

addition of 10 μL of stop reaction solution (50 mM EDTA in formamide) prior to analysis by 16% denaturing PAGE.

Acknowledgment. Dedicated to Professor Kelvin Kenneth Ogilvie on the occasion of his 65th birthday. We thank the Canadian Institute of Health Research (CIHR), the National Science & Engineering Council of Canada (NSERC), and McGill University for funding. We thank J. K. Watts and R. A. Donga for critical proofreading of the manuscript. M.J.D. is the 2007 recipient of the Bernard Belleau Award (Canadian Society for Chemistry).

Supporting Information Available: Figures and tables as described in the text. This material is available free of charge via the Internet at http://pubs.acs.org.

JA071336C